Temperature-dependent thermal conductivity in low-dimensional lattices

1990 J. Phys.: Condens. Matter 2 7575

(http://iopscience.iop.org/0953-8984/2/37/003)

J. Phys.: Condens. Matter 2 (1990) 7575–7584. Printed in the UK

Temperature-dependent thermal conductivity in low-dimensional lattices

Norihiko Nishiguchi and Tetsuro Sakuma
Department of Engineering Science, Hokkaido University, Sapporo 060, Japan

Received 13 March 1990

Abstract. The validity of Fourier's law is investigated by taking account of the temperature dependence of the thermal conductivity for the one- and two-dimensional diatomic lattices. The thermal conductivity is found to be proportional to the inverse of temperature for both the one- and two-dimensional lattices. Fourier's law is confirmed by excluding the non-diffusive or ballistic energy flow from the total energy current.

1. Introduction

Heat transport in an electrically insulating material is attributed to the lattice vibrations and is described in terms of the phenomenological theory referred to as Fourier's law. A number of simulations using molecular dynamics has been performed to verify Fourier's law in low-dimensional lattices from first principles [1–6]. They were devoted to showing that the magnitude of the thermal conductivity was independent of system size and most attempts failed to present the normal thermal conductivity without external disturbances [6]. This series of disappointing results were reviewed by Visscher [7] and by MacDonald and Tsai [8].

Recently Mokross and Büttner [9] exhibited that the thermal conductivity does not depend on the lattice size in a one-dimensional diatomic Toda lattice. Using a similar method, Jackson and Mistriotis [10] tried to confirm evidence of Fourier's law for much longer diatomic Toda lattices than those used by Mokross and Büttner and showed that the size-dependence of the thermal conductivity disappeared for lattices whose size is greater than 250 atoms. They also exhibited that the pulse–pulse collisions play dominant roles in the energy sharing mechanism.

Although the previous works seemed to present successfully the normal thermal conductivity [9, 10], the estimated magnitudes of the thermal conductivity could not be considered to be the correct ones. If the systems could offer the normal thermal conductivity, the thermal conductivity has to be temperature dependent as is known in a real material [11]. The temperature dependence has not been seriously considered so far, although there exists evidence of the deviation from the linear temperature-profile in the numerical experiments. In cases of long lattices with large temperature differences between lattice ends, concave temperature profiles have been seen [5, 9, 10], however, they were approximated with straight lines to evaluate the thermal conductivity. We assert that the bending temperature profile is related to the temperature dependence of the thermal conductivity and that it should be taken into account in investigating Fourier's law.

0953-8984/90/377575 + 10 $03.50

We note here that the bending temperature profile is not an unrealistic phenomenon. In the steady, non-equilibrium state, the time-averaged heat current must be constant through the system. Therefore if the thermal conductivity depends on the local temperature, the temperature gradient should vary with the temperature or the lattice position. This leads naturally to the non-linear temperature profile. The temperature-dependent thermal conductivity of the two-dimensional lattices was studied by Mountain and MacDonald by means of molecular dynamics [12]. However, their criterion for the establishment of the steady, non-equilibrium state was the appearance of a linear temperature profile. This is not self-consistent for the temperature-dependent thermal conductivity because there is no longer a steady current independent of the lattice position. Therefore, the heat current must be constant through the system for the steady, non-equilibrium state. The change in the temperature profile is expected to reflect the structural characteristics of the relevant system.

Another troublesome phenomenon due to the large temperature difference of heat reservoirs is that the energy may not only be transferred by a diffusion process [5, 10]. As the net non-diffusive or ballistic energy flow increases with the temperature difference between the heat reservoirs, the evaluation of thermal conductivity by means of the crude observed-heat currents does not give the correct results. Then, we have to exclude the contribution of the non-diffusive part from the heat current in order to investigate the thermal conductivity.

In this paper, we study the validity of Fourier's law for the one- and two-dimensional Toda lattices using molecular dynamics techniques. We take account of the non-linear temperature profiles and of the non-diffusive energy flow to estimate the thermal conductivity. In addition to the size-independent magnitude of the thermal conductivity, we employ another criterion for the validity of Fourier's law that the thermal conductivity should be expressed with the same function of the temperature in different temperature regions. We, therefore, examine the system with different sizes in various temperature regions.

The plan of this paper is as follows: in section 2, we give a brief description for the two kinds of non-linear lattices, one of which is the one-dimensional diatomic Toda lattice and the other is the two-dimensional diatomic Toda lattice. Details of numerical simulation are also described in this section. As we examine the system over a wide range of temperature, there is a question as to whether the system can exhibit dynamical irreversibility at very low temperatures. In section 3, we investigate the dynamical behaviour over a short time period which is essential to the thermodynamic behaviour. The resultant temperature profiles are analysed and fitted with an empirical formula of the exponential type in section 4. In section 5, we estimate the heat currents from the measurements. The heat currents are assumed to consist of the ballistically propagating energy flow and the normal one which is expected to obey Fourier's law. The temperature dependence of the thermal conductivity is derived from the numerical result in which the heat current is constant through the system. The magnitude of the thermal conductivity is estimated by excluding the ballistic energy currents from the total heat currents. The resultant thermal conductivity becomes proportional to the inverse of the local temperature and the magnitude is independent of the lattice sizes. The last section will be devoted to the summary and discussions.

2. One- and two-dimensional diatomic Toda lattices and numerical simulations

As the one-dimensional diatomic Toda lattice is well known [7, 8], we begin this section with the two-dimensional Toda lattice referred to as Mikhailov's lattice [13] which is

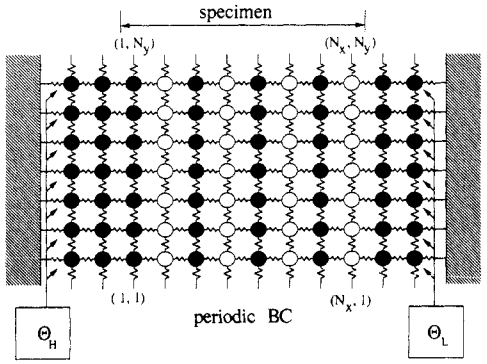

Figure 1. Model and experimental situation for the two-dimensional lattice. Full and open circles denote the atoms with masses m_0 and m_1 of the specimen lattice, respectively. The grey circles denote the atoms with mass m_0 in the buffer areas. All particles are connected with Toda potentials along the x direction and harmonic potentials along the y direction. The periodic boundary condition is used for the displacement along the y direction. The lattice is heated by the elastic collisions of atoms between the lattice ends and the heat reservoirs whose temperatures are θ_H and θ_L.

obtained by arranging N_y one-dimensional Toda lattices with N_x atoms in lines and by connecting atoms side by side with nearest-neighbour harmonic potentials. This lattice is found to be analytically integrable [13] as is the one-dimensional Toda lattice. Here we restrict the displacement of the atoms to be scalar. It is easily understood that the system is reduced to the one-dimensional Toda lattice if we put $N_y = 1$. In order to introduce the non-integrability into the system, we modify the mass configuration by putting two kinds of masses on the lattice sites as follows:

$$m_{ij} = \begin{cases} m_0 & \text{for even } i \\ m_1 & \text{for odd } i \end{cases} \tag{1}$$

for any j, where the subscripts i and j denote the position in the lattice in the x- and y-direction, respectively. In the numerical experiments, large temperature discontinuities are observed at the interfaces between the heat reservoirs and the specimen lattice. This phenomenon has been referred to as thermal boundary resistance or Kapitza resistance due to a large mismatch in acoustic impedance between them [14]. As it strongly deforms the temperature profile in the vicinity of the interfaces, we put mono-atomic lattices as buffer areas between the heat reservoirs and the specimen lattice. The temperatures of these buffer areas are almost constant in each area and are well-defined experimentally as seen below. We set the mass of the buffer areas to be m_0. In what follows, we set $m_0 = 1$ and $m_1 = 0.5$. Figure 1 shows the mass configuration for the diatomic Mikhailov's lattice.

As can be seen in figure 1, N_x and N_y denote the size of the specimen lattice and each buffer area has atomic length N_x'. Then our system has the total atomic length $N (= N_x + 2N_x')$. We set $N_x' = 10$ throughout the present experiments. Due to the restriction of the computer capacity, N_y is set to be 10. The length of the specimen lattice N_x varies in the range from 250 to 450.

The total energy for this system is written by

$$H = \sum_{i}^{N} \sum_{j}^{N_y} \left\{ \frac{p_{ij}^2}{2m_{ij}} + V(u_{ij} - u_{i-1j}) + U(u_{ij} - u_{ij-1}) \right\} + \text{interaction with heat reservoirs} \tag{2}$$

where p_{ij} and u_{ij} are the momentum and displacement of the atom at (i, j) sites, respectively. The potential function $V(r)$ is a Toda potential such as

$$V(r) = (b/a) \exp(-ar) + br - (b/a) \tag{3}$$

and the harmonic potential $U(r)$ is expressed as

$$U(r) = (c/2)r^2. \tag{4}$$

a, b and c are the potential parameters which are all set to unity in this paper. A periodic

boundary condition is used for the displacement of the end column atoms, i.e. $u_{i,1} = u_{iN_y+1}$.

The atoms linked to the fixed walls with the anharmonic potentials interact impulsively with heat reservoirs with prescribed temperatures at θ_H and θ_L, respectively. The energy is exchanged through elastic collisions of the end atoms with gas particles in the reservoirs. The gas particles have the Maxwell distribution in velocity of the form

$$N(v, \theta) = \sqrt{M/2\pi k_B \theta}\, \exp(-Mv^2/2k_B\theta) \tag{5}$$

where M is the mass of gas particles which is set to unity in these experiments. Here θ and k_B are the temperature of the heat reservoir and the Boltzmann constant, respectively. In the present work, k_B is set to unity.

The equation of motion is numerically solved by means of the Runge–Kutta–Gill method. The time inverval δt is chosen so that the computational errors in the total energy conservation are suppressed within 0.1% of the total energy through the experiments. The magnitude of the time interval depends on the temperature region of the numerical experiments and becomes of the order of 10^{-3} to 10^{-2} in our case.

3. Local rate of divergence of trajectories and temperature region with stochastic behaviour

If the system obeys Fourier's law whose thermal conductivity has the temperature dependence, the thermal conductivity should be expressed with a function of temperature. The function must be the same formula in different temperature regions where the system exhibits irreversibility enough for the normal thermal conductivity. This is the other criterion of the validity of Fourier's law. Then we examine the system in several temperature regions to be distinguished in terms of pairs of temperatures of heat reservoirs where the ratio θ_H/θ_L is set to equal 4. In what follows, we refer to them as A, B, C, D and E which denote ($\theta_H = 2$, $\theta_L = 0.5$), ($\theta_H = 10$, $\theta_L = 2.5$), ($\theta_H = 20$, $\theta_L = 5$), ($\theta_H = 40$, $\theta_L = 10$) and ($\theta_H = 80$, $\theta_L = 20$), respectively.

As the non-linearity is reduced effectively with lowering temperature, there is a possibility that the system no longer exhibits the irreversibility at very low temperatures. The normal thermal conductivity is not expected in such a temperature region. Therefore, it is necessary to investigate the critical temperature for the transition from infinite to finite thermal conductivity.

The stochastic behaviour is believed to be related to the irreversibility and the divergence of trajectories starting from the close points in phase space has often been investigated for quantitative discussions. In the thermal equilibrium state, we describe the rate of divergence by means of Lyapunov characteristic exponents. As noted by Jackson and Mistriotis [10], on the other hand, the dynamical behaviour in a short time interval, which is characteristic to the system, is essential to the thermodynamic behaviour in the non-equilibrium state. The time interval was taken to be the sound-transit time across the system. According to them, even a non-integrable system would not exhibit irreversibility within a characteristic time interval shorter than that of the loss of correlation between initial and final positions in the phase space. How fast the correlation is lost depends on the effective strength of the non-linearity or the temperature of the system. We, therefore, try to investigate the divergence of trajectories in the short time interval for various values of the energy of the system. We employ the method developed by Jackson and Mistriotis [10] to test the rate of the

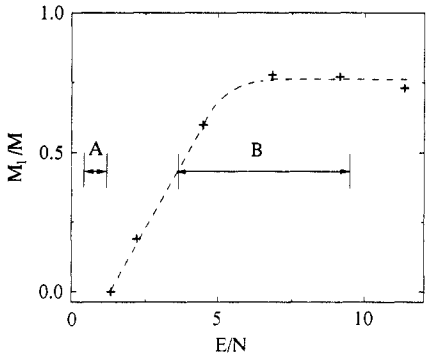

Figure 2. The probability that the system exhibits the stochastic behaviour within the short time interval as a function of the energy per atom. The examined system is the diatomic Toda lattice with $N = 30$. The characteristic time interval is $T_s = 25$.

divergence. The examined system is the one-dimensional diatomic Toda lattice without the buffer areas. The lattice size is 30 atoms for computational convenience. The sound-transit time, T_s, is determined to be 25 from the pulse and wave propagation experiments. Since the rate depends on the position in the phase space, we therefore try more than one hundred measurements of the local rate of divergence for each energy. The type of divergence is judged from the value of $\mu(T_s)$ which is defined by

$$\mu(T_s) = \int_0^{T_s} dt \{|d(t) - A(q_\Gamma, p_\Gamma, T_s) \exp(k(q_\Gamma, p_\Gamma, T_s)t)|^2 - |d(t) - B(q_\Gamma, p_\Gamma, T_s)t - C(q_\Gamma, p_\Gamma, T_s)|^2\}. \tag{6}$$

Here, the notations of equation (6) are the same as those used in [10]. If $\mu < 0$, the divergence is considered to be exponential with time. We perform this test numerically and the ratios of the number of the exponential development of the distance with time, M_1, to the total trials, M, versus the energy per site, E/N, are plotted in figure 2. Below $E/N = 1.33$, the ratio becomes zero. The local rates increase with increasing energy and saturate above $E/N = 5$. We show the tendency with a broken curve. The broken curve is the lower limit and the system is expected to exhibit the irreversibility above $E/N = 1.33$ in the thermodynamic limit ($N \to \infty$). Although the temperature does not coincide exactly with the energy per atom, as shown in the following section, the magnitudes are comparable to each other. We then roughly estimate the critical temperature from infinite to finite thermal conductivity to be 1.33. The regions labelled A and B are the temperature regions of the specimen lattices, which will be discussed in the next section.

4. Temperature profiles

We define the local temperature to be twice as large as the total-time-average of the local kinetic energy. The temperature profile along the x direction of the lattice is obtained by averaging the local temperature over the lattice width.

$$T_i = 2\left\langle \frac{1}{N_y} \sum_{j=1}^{N_y} \frac{p_{ij}^2}{2m_{ij}} \right\rangle_t. \tag{7}$$

Here $\langle\ \rangle_t$ denotes the total-time-average. Figures 3(*a*) and (*b*) exhibit the temperature profiles of the one- and two-dimensional lattices, respectively. Both figures show the exponential decrease of the temperature with lattice positions. As we are keeping the

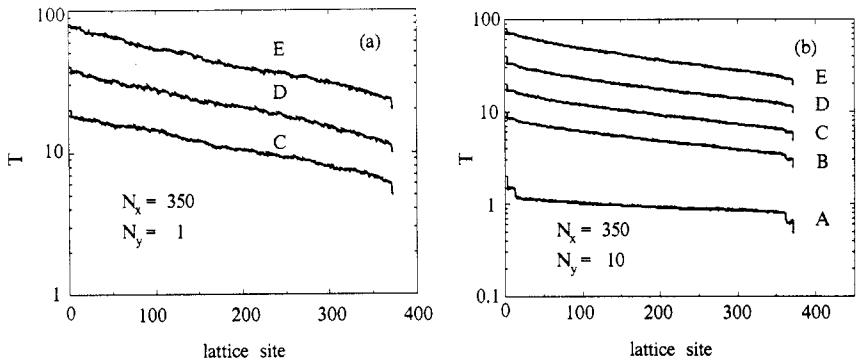

Figure 3. (*a*) Temperature profiles for the one-dimensional diatomic Toda lattice. The length of the specimen lattice is 350 atoms. C, E and D denote the temperature regions explained in the text. (*b*) Temperature profiles for two-dimensional diatomic Toda lattice. The lattice is of size $N_x = 350$ and $N_y = 10$. The temperature profiles are plotted from a very low temperature region, A, to a high one, E.

ratio of the temperatures of the heat reservoirs constant, the temperature profiles become parallel as seen in figures 3(*a*) and (*b*) except the data for the temperature region A. As is easily understood from the discussion in the previous section, the system cannot exhibit the irreversibility below the critical temperature corresponding to the energy $E/N = 1.33$. This is the reason why the temperature gradient in the region A is distinguished from those in the high temperature regions. In what follows, we use the two-dimensional lattices to investigate the heat conduction at low temperatures.

Though we plot the resultant temperature profiles only for $N_x = 350$, we have quite similar temperature profiles for $N_x = 250$ and 450 for both the one- and two-dimensional cases. As mentioned above, the temperature profiles exhibit exponential decrease from the end of the lattice for both dimensional lattices. We can, therefore, approximate the temperature profile independently of dimensionality with the exponential function of the form

$$T(x) = T_H(T_L/T_H)^{x/N_x} \tag{8}$$

where T_H and T_L are not the temperatures of the heat reservoirs but are those at the ends of the specimen lattice and x measures the distance from the interface between the buffer area and the specimen lattice. Here we use x instead of subscript i, for convenience. The magnitudes of T_H and T_L are estimated by the least-square method. Therefore, T_H and T_L do not exactly coincide with the observed values because of the thermal boundary resistance. In terms of the empirical formula for the temperature profile (8), the temperature gradient yields

$$dT/dx = -(1/N_x)\ln(T_H/T_L)T. \tag{9}$$

5. Normal heat currents and thermal conductivity

The heat current along the x direction is an observable of interest, too, and is derived from the local energy conservation. The local energy of an atom at site (i, j) is written as

$$\varepsilon_{ij} = p_{ij}^2/2m_{ij} + \tfrac{1}{2}[V(u_{ij} - u_{i-1j}) + U(u_{ij} - u_{ij-1})] + \tfrac{1}{2}[V(u_{i+1j} - u_{ij}) + U(u_{ij+1} - u_{ij})] + \text{interaction with the reservoirs.} \tag{10}$$

Hereafter, let $J(ij; kl)$ stand for the energy current from (ij) site to (kl). The energy current obeys the following difference equation implying the local energy conservation law.

$$J(i+1j; ij) - J(ij; i-1j) + J(ij+1; ij) - J(ij; ij-1) + \partial \varepsilon_{ij}/\partial t = Q_{Hj}\delta_{i,1} + Q_{Lj}\delta_{i,N_x}. \tag{11}$$

Q_{Hj} and Q_{Lj} in the right-hand side of equation (11) are the exchanged energies per unit time with the heat reservoirs of high and low temperature, respectively. Because the energy transfer takes place through the interatomic potentials, only the energy flow between the adjacent sites is allowed. As we are interested in the heat flow along the x direction, we extract the relevant heat flow from equation (11) by averaging the equation over the lattice width under the periodic boundary condition $J(i0; i1) = J(iN_y; iN_y + 1)$. Summing up the equations with respect to i up to k yields

$$\frac{1}{N_y}\sum_{j=1}^{N_y} J(k+1j; kj) = \frac{1}{N_y}\sum_{j=1}^{N_y} J(1j; 0j) - \frac{1}{N_y}\sum_{i=1}^{k}\sum_{j=1}^{N_y}\frac{\partial \varepsilon_{ij}}{\partial t} + \frac{1}{N_y}\sum_{j=1}^{N_y} Q_{Hj}. \tag{12}$$

We define the heat current $J_x(k+1; k)$ along the x direction by taking different kinds of time average of equation (12) from the total-time-average to be discussed below

$$J_x(k+1; k) = \frac{1}{N_y}\sum_{j=1}^{N_y}\langle J(1j; 0j)\rangle - \frac{1}{N_y}\sum_{i=1}^{k}\sum_{j=1}^{N_y}\left\langle\frac{\partial \varepsilon_{ij}}{\partial t}\right\rangle + \frac{1}{N_y}\sum_{j=1}^{N_y}\langle Q_{Hj}\rangle. \tag{13}$$

It should be noted here that the angle brackets do not have the subscript t for the distinction from the total-time-average. The first term in the right-hand side is the heat flow from the fixed wall to the first row atoms after which it is expected to vanish. The second one does not contribute to the heat current in a steady non-equilibrium state where the steady temperature profile is established. Therefore, the current no longer has the site dependence after the establishment of the steady state. We check the heat currents at five lattice positions referred to as α, β, γ, δ and ε. The points α and ε are located at the interface between the heat reservoirs with high and low temperatures, and the others β, γ and δ are at $N/4$, $N/2$ and $3N/4$ measured from the point α, respectively.

Instead of the total-time-average, we define the time-average of the heat flow as follows:

$$\langle J\rangle = \frac{1}{\tau_1}\left(\int_0^{\tau+\tau_1} J(t)\,\mathrm{d}t - \int_0^{\tau} J(t)\,\mathrm{d}t\right) \tag{14}$$

where $J(t)$ means the right-hand side of equation (12). Here τ is taken to be as large as possible so that the site dependence of $\langle J\rangle$ may disappear. We plot the heat currents from equation (13) for the two-dimensional lattice in figure 4. In this case, τ_1 is taken to be 3×10^5 steps. The five heat currents observed coincide with each other in magnitude to an accuracy of 0.3%. The steady state is clearly established. The time-averaged magnitude of the heat currents becomes 1.212×10^{-2}. The fluctuation width becomes 12% of the averaged magnitude in this case. The fluctuation widths are larger in the one-dimensional case than those in the two-dimensional case. The advantage of this time-averaging method is to obtain the magnitude precisely in a shorter computational time than the total-time-averaging case since the heat currents gather proportionally to the inverse of computational time in the latter case. For the temperature profiles, we use the total-time-average because the profile is not sensitive to the averaging method.

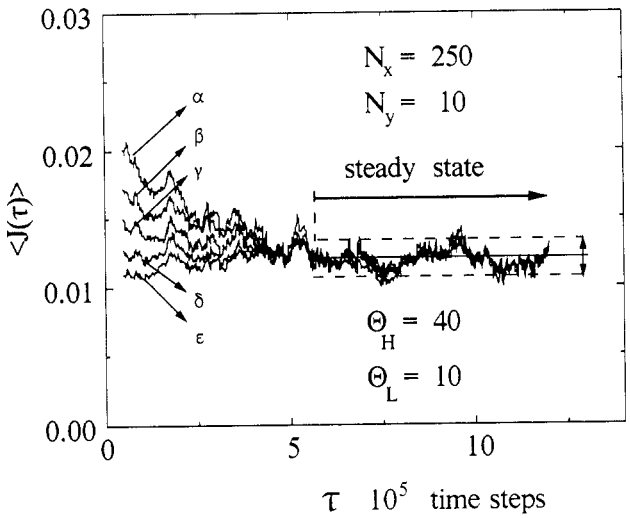

Figure 4. Heat currents versus time steps for the two-dimensional lattice with $N_x = 250$ and $N_y = 10$. The temperatures of the heat reservoirs are $\theta_H = 40$ and $\theta_L = 10$. The Greek letters denote the positions for the observation of the heat currents in the lattice. α and ε are at the interface between the heat reservoir with high and low temperature, and β, γ and δ are located at $N/4$, $N/2$ and $3N/4$ measured from α, respectively.

Here we write the heat current J_x as

$$J_x = J_N + J_B. \tag{15}$$

The first term of the right-hand side is the normal heat current due to the local temperature gradient and the other is the ballistic or non-diffusive part. The normal heat current J_N is expected to obey the following Fourier law

$$J_N = -\kappa \, \mathrm{d}T/\mathrm{d}x. \tag{16}$$

Here we assume that the ballistic energy flow depends on the temperature difference of the buffer areas and on the system size since the buffer areas effectively act as the heat baths. The temperatures of the buffer areas $T_{B,H}$ and $T_{B,L}$ are slightly larger and smaller than T_H and T_L, respectively, because of the thermal boundary resistance.

Substituting equations (9) and (16) into (15) yields

$$J_x = \kappa \, (1/N_x) \log(T_H/T_L)T + J_B(T_{B,H} - T_{B,L}, N_x). \tag{17}$$

Equation (17) gives the temperature dependence of the thermal conductivity. Although the temperature distributes between T_H and T_L, the measured heat currents are independent of the temperature in the steady, non-equilibrium state as discussed above. Therefore, the thermal conductivity must be proportional to the inverse of the temperature to cancel out the temperature dependence of the first term of the right-hand side of (17). Then we can write the thermal conductivity as follows:

$$\kappa = \xi/T \tag{18}$$

where ξ is a constant.

The question arises as to whether the thermal conductivity defined by equation (18) is an intensive quantity or whether ξ is independent of the system size. In order to

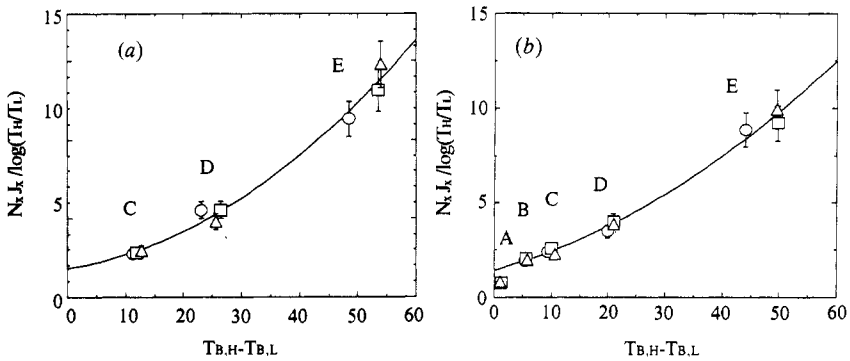

Figure 5. The heat current per unit length/$\log(T_H/T_L)$ versus temperature difference of the buffer areas. Open circles, squares and triangles denote the data for the lattices with N_x = 250, 350 and 450, respectively. The full curve is drawn with the least-squares method to exhibit the extrapolation of the data to zero temperature difference. (*a*) Represents the one-dimensional Toda lattice, and C, D and E denote the temperature regions to be observed. The extrapolated magnitude of ξ becomes 1.83. (*b*) Represents the two-dimensional diatomic Toda lattice, and A, B, C, D and E denote the temperature regions to be observed. The extrapolated magnitude of ξ becomes 1.44.

estimate ξ from the measurements, we have to exclude the contribution of the ballistic heat current from (17). If we could take the limit of the temperature difference to zero whilst keeping the ratio T_H/T_L constant, we would obtain the normal heat current in the limit. However, the very low temperature experiment cannot give the normal heat current because the irreversibility is not expected in such a temperature region. Therefore, we extrapolate ξ from the experimental data in the high temperature regions. Substituting equation (18) into (17) yields

$$J_x N_x/\log(T_H/T_L) = \xi + J_B(T_{B,H} - T_{B,L}, N_x)N_x/\log(T_H/T_L). \tag{19}$$

Figures 5(*a*) and (*b*) show the results for the one- and two-dimensional lattices, respectively. As the temperature difference decreases, the magnitude of $J_x N_x/\log(T_H/T_L)$ decreases drastically and seems to become positive and achieve a finite value at zero temperature difference. In addition, it should be noted that the results are almost size-independent. These facts say that the normal current exists and that the ξ is invariant for all the experiments. That is, we can conclude that Fourier's law is satisfied in the one- and two-dimensional lattices. The value of ξ yields 1.83 and 1.44 for the one- and two-dimensional lattices, respectively, from the figures. Here, we excluded the data of temperature region A for the estimation of ξ.

We note here that the data of A deviate from the extrapolated full curve. This is quite reasonable because the system does not exhibit the stochastic dynamical motions in this temperature region and there is only the ballistic component in the heat current present which vanishes at the zero temperature difference.

6. Summary and discussion

In this paper, we examined the heat transport in the one- and two-dimensional nonlinear lattices for testing the validity of Fourier's law in terms of molecular dynamics. We paid special attention to the bending of the temperature profiles in the lattice which

had been overlooked by many authors and attributed the deviation from the linear temperature distribution to the temperature dependence of the thermal conductivity. The temperature profiles were investigated in detail and approximated well with the exponential function for both the one- and two-dimensional lattices. Substituting the specified temperature profile into the definition of thermal conductivity leads to the temperature-dependent thermal conductivity which is proportional to the inverse of the temperature. This behaviour is quite similar with that in a real material at high temperatures where the anharmonic interatomic potential plays an essential role in the heat transport in the solid.

For the existence of Fourier's law, the coefficient ξ of thermal conductivity must be an intensive quantity. That is, the coefficient has to be independent of system size. Excluding the ballistically propagating heat flow from the measured currents, we obtained ξ to be independent of the system size. This is the evidence of the validity of Fourier's law in the relevant lattices.

To investigate the temperature region where the normal thermal conductivity was expected, we examined the dynamical behaviour in the short time interval. We judged the type of the local rate of divergence of trajectories, whether it was linear or exponential with time. From the measure of the establishment of the irreversibility, M_1/M, we found the critical temperature to be $T_c = 1.33$, which indicates the transition from infinite to normal thermal conductivity. This result agrees with the temperature-region dependence of the temperature profiles and of the normal heat currents. Below the critical temperature, the gradient of the temperature profiles becomes quite small and the normal heat flow is drastically reduced. The reduction of the normal heat flow means also that the system does not exhibit the stochastic behaviour.

Finally, we emphasise again that we should take account of the non-linear temperature profile and the existence of the ballistic heat current to estimate the thermal conductivity.

Acknowledgments

The authors would like to thank M Nagao and T Yamanaka for their computational help. One of us (NN) acknowledges financial support by The Foundation HATTORI-HOKOKAI.

References

[1] Matsuda H and Ishii K 1970 *Prog. Theor. Phys. Suppl.* **45** 56
[2] Nakagawa H 1970 *Prog. Theor. Phys. Suppl.* **45** 231
[3] Toda M 1979 *Phys. Scr.* **20** 424
[4] Payton D N, Rich M and Visscher M W 1967 *Phys. Rev.* **160** 706
[5] Mareschal M and Amellal A 1988 *Phys. Rev.* A **37** 2189
[6] Rich M and Visscher W M 1975 *Phys. Rev.* B **11** 2164
[7] Visscher W M 1976 *Methods Comput. Phys.* **15** 371
[8] MacDonald R A and Tsai D H 1978 *Phys. Rep.* **46** 1
[9] Mokross F and Büttner H 1983 *J. Phys. C: Solid State Phys.* **16** 4539
[10] Jackson E A and Mistriotis A D 1989 *J. Phys.: Condens. Matter* **1** 1223
[11] For a review see Carruthers P 1961 *Rev. Mod. Phys.* **33** 92
[12] Mountain R D and MacDonald R A 1983 *Phys. Rev.* B **28** 3022
[13] Mikhailov A V 1979 *JETP Lett.* **30** 414
[14] Khalatnikov I M 1952 *Zh. Eksp. Teor. Fiz.* **22** 687; 1965 *Introduction to the Theory of Superfluidity* (New York: Benjamin) ch 23 p 138